Insight into the Molecular Properties of Chitlac, a Chitosan Derivative for Tissue Engineering

ARTICLE *in* THE JOURNAL OF PHYSICAL CHEMISTRY B · SEPTEMBER 2013

Impact Factor: 3.3 · DOI: 10.1021/jp4067263 · Source: PubMed

9 AUTHORS, INCLUDING:

Carmen Esteban
Universidad Nacional de San Luis
8 PUBLICATIONS **17** CITATIONS
SEE PROFILE

Anna Coslovi
Novartis Vaccines
15 PUBLICATIONS **223** CITATIONS
SEE PROFILE

Julio Benegas
Universidad Nacional de San Luis
72 PUBLICATIONS **492** CITATIONS
SEE PROFILE

Ivan Donati
Università degli Studi di Trieste
69 PUBLICATIONS **1,489** CITATIONS
SEE PROFILE

THE JOURNAL OF PHYSICAL CHEMISTRY B

Article

pubs.acs.org/JPCB

Insight into the Molecular Properties of Chitlac, a Chitosan Derivative for Tissue Engineering

Nicola D'Amelio,*[,†,‡,#] Carmen Esteban,[§] Anna Coslovi,[∥,▽] Luigi Feruglio,[†] Fulvio Uggeri,[⊥] Myriam Villegas,[§] Julio Benegas,[§] Sergio Paoletti,[∥] and Ivan Donati[∥]

[†]Bracco Imaging SpA-CRB Trieste, AREA Science Park, Building Q, SS 14, km 163.5, 34149 Basovizza (Trieste), Italy

[‡]CBM S.r.l. - Consorzio per il Centro di Biomedicina Molecolare, AREA Science Park, SS 14, km 163.5, 34012 Basovizza (Trieste), Italy

[§]Instituto de Matematica Aplicada San Luis (IMASL), Department of Physics, National University of San Luis/CONICET, Avenida Ejército de los Andes 950, D5700HHW San Luis, Argentina

[∥]Department of Life Sciences, University of Trieste, via L. Giorgieri 5, 34127 Trieste, Italy

[⊥]Bracco Imaging SpA, via E. Folli 50, 20134 Milano, Italy

Supporting Information

ABSTRACT: Chitlac is a biocompatible modified polysaccharide composed of a chitosan backbone to which lactitol moieties have been chemically inserted via a reductive N-alkylation reaction with lactose. The physical−chemical and biological properties of Chitlac that have been already reported in the literature suggest a high accessibility of terminal galactose in the lactitol side chain. This finding may account for its biocompatibility which makes it extremely interesting for the production of biomaterials. The average structure and the dynamics of the side chains of Chitlac have been studied by means of NMR (nuclear Overhauser effect and nuclear relaxation) and molecular dynamics to ascertain this hypothesis. A complete assignment of the ^{1}H and ^{13}C NMR signals of the modified polysaccharide has been accomplished together with the determination of the apparent pK_a values of the primary and secondary amines (6.69 and 5.87, respectively). NMR and MD indicated a high mobility of Chitlac side chains with comparable average internuclear distances between the two techniques. It was found that the highly flexible lactitol side chain in Chitlac can adopt two distinct conformations differing in the orientation with respect to the polysaccharide chain: a folded conformation, with the galactose ring parallel to the main chain, and an extended conformation, where the lactitol points away from the chitosan backbone. In both cases, the side chain resulted to be highly hydrated and fully immersed in the solvent.

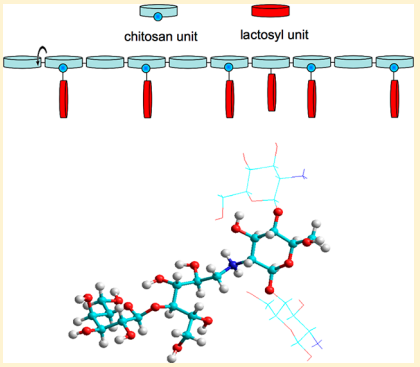

INTRODUCTION

Chitosan is a collective name for the linear polysaccharides derived from deacetylation of chitin, the structural component of fungal cell walls and exoskeleton of arthropods. Chemically, they are composed of β-1→4 linked glucosamine units, with some residual interspersed *N*-acetyl-glucosamine residues: the former residues endow the polysaccharide with positively charged groups characterized by a pK_a of ∼6.6 at 25 °C at physiological ionic strength.[1] Availability, absolute safety for medical use, and biodegradability make chitosan very interesting for tissue engineering and biomaterials design.[2,3]

Although biotechnologically relevant, chitosan can be further improved from the point of view of the bioactive features and tuned as to the physical−chemical behavior. As an example, modification of chitosan with oligosaccharide pendant groups does alter its solubility at physiological pH. Strand et al. reported an increased transfection on HEK293 cells upon modifying chitosan by introducing a trisaccharide as a side chain and by self-branching of modified chitosans.[4]

The modification of chitosan backbone with lactose moieties traces back to the late 1980s, with the work by Yalpani and coworkers that established the chemical conditions for the modification of the polysaccharide chain and explored, to some extent, its rheological features.[5] Some of the present authors have reinvestigated the synthesis of a lactose-modified chitosan, that has been named Chitlac, and its biological significance in terms of ligand−receptor interactions with lectins. Chitlac was found to engage an integrin on the surface of chodrocytes via a bridging lectin, that is, Galectin-1,[6] which specifically recognizes the galactose pending groups flanking the chitosan backbone. Galectin-1 is a highly conserved member of the family of galactose-binding proteins.[7] It is a homodimer of 28 kDa with a carbohydrate recognition domain (CRD), which preferentially binds to Galβ(1→4)GlcNAc sequences present in N-linked and in O-linked glycans.[8] Recognition of a carbohydrate sequence

Received: July 8, 2013
Revised: September 23, 2013
Published: September 30, 2013

dx.doi.org/10.1021/jp4067263 | J. Phys. Chem. B 2013, 117, 13578−13587

by Galectin-1 has been considered as the key step for several biological events like, among several others, cell adhesion, growth, and regulation.[9−11] As an extracellular effector, Galectin-1 binds to laminin, fibronectin, and elastin[12] in the extracellular matrix, which is fundamental to maintain tissue homeostasis, composition, reorganization, and mechanical performance. Galectin-1 displays multivalent binding to glycoconjugates and cross-linking abilities.[13]

The interaction between Chitlac and Galectin-1 triggers the aggregation of porcine articular chondrocytes, which is accompanied by an increased production of glycosaminoglycans.[14] Moreover, Chitlac was found to have cell-stimulating effects also on bone cells[15] and, due to the ubiquitous presence of Galectins, it might play an important role in several other cell types.

In addition to the specific bioactive features, the presence of the lactitol moieties on the side chain endows the modified polysaccharide with a high solubility at physiological pH. Under these conditions and in aqueous NaCl 0.15 M, Chitlac is even miscible with alginate and hyaluronan (HA).[16] Indeed, binary solutions and hydrogels have been prepared and showed synergistic polyanion−polycation interactions.[17] When binary hydrogels were considered, the presence of the bioactive component (Chitlac) led to a notable increase in the proliferation of encapsulated porcine chondrocytes when compared with microbeads composed of alginate alone.[18]

The biochemical characteristics of Chitlac are certainly influenced by the structural disposition of the oligosaccharide side chains in the aqueous solvent. In particular, the possibility for the ligand to engage the receptors is strongly dependent on the accessibility of the galactose terminal and on the overall conformational properties of Chitlac.

The structural analysis of oligo- and polysaccharides is very challenging for their intrinsic flexibility, which represents experimentally and theoretically a main bottleneck for high-resolution structure determination.[19] In that regard, and of particular interest for this work, it is noted that NMR and computational approaches have been recently used for the determination of the local conformation and dynamics of HA, accounting for the polymer hydrodynamic properties and its interactions with proteins.[20] Besides this example, a residue-specific conformation and inherent dynamics analysis still remains a challenge for polysaccharides, especially when very flexible side chains are involved. In the present paper, NMR and molecular dynamics have been exploited to elucidate the structural and conformational characteristics of the side chain of Chitlac, that is, the flanking galactose-bearing moieties.

EXPERIMENTAL SECTION

Chitosan (residual degree of acetylation = 11.3%) was purchased from Sigma-Aldrich (Milwaukee, WI) and purified by precipitation with isopropanol, followed by a dialysis against deionized water. The molecular weight of chitosan was found to be around 600 000.[14] Chitlac samples with various degrees of lactosylation (namely, 18, 36, 50, and 58%, based on the Chitosan repetitive units) were synthesized from purified chitosan according to a procedure previously reported.[14] Table 1S of Supporting Information section reports the chemical characteristics of the Chitlac samples prepared in the present study.

Differential Scanning Calorimetry. Differential scanning calorimetry (DSC) measurements were performed with a DSC Q-100 (TA Instrument, USA). Approximately 2 mg of freeze-dried chitlac was crimped in a standard aluminum pan and heated gradually from 0 to 250 °C at a heating constant rate of 10 °C/min under constant purging of nitrogen at a rate of 50 mL/min.

Thermogravimetric Analysis. Thermogravimetric analysis (TGA) was performed with a TGA Q500 (TA Instrument, USA). The sample was heated in the temperature range 20−650 °C with a heating rate of 10 °C/min under a constant purging of nitrogen at a rate of 10 mL/min.

Bacterial Growth Inhibition. Bacterial growth inhibition was measured with a microtiter plate reader (Tecan Trading AG, Switzerland). 200 μL of bacterial suspension (*S. aureus* ATCC 25923) at a concentration of 1×10^6 cells/mL in 20% Muller−Hinton broth in the absence or in the presence of chitlac was placed on the wells. Plates were incubated for 37 °C for 4 h under stirring; the bacterial growth was monitored by measuring the Optical Density at 620 nm.

NMR Resonance Assignment. Full resonance assignment of nonexchangeable protons and carbons was accomplished by means of 2D-^{1}H,^{1}H-TOCSY-^{1}H,^{13}C-HSQC, 2D-COSY, and 2D-NOESY spectra. NMR spectra were typically performed on samples at a concentration of 10 mg/mL, pH 7, and 300 K. NOESY experiments for structure calculations were performed in D_2O (pD 4) at all lactosylation degrees.

Because backbone protons display very broad peaks and are invisible in 2D-^{1}H,^{13}C HSQC spectra, their assignment was accomplished by comparison to chitosan solutions in the same concentration and pH conditions.

Relaxation measurements were performed at a concentration 6 mM in terms of polymer repeating units for all cases analyzed. The pD was adjusted to 3.5 using a 25 mM phosphate buffer to ensure the protonation of all amine groups.

For the pK_a determination, samples in H_2O (10% D_2O) were prepared at various pH values (in the range between 1.9 and 12) to identify exchangeable protons.

NMR Structure Calculation. Interproton distances (d) were calculated from 2D-NOESY cross peak intensities (V) measured on samples at a concentration of 6 mM in terms of polymer repeating units by means of eq 1. H_{12} geminal protons were used as reference distance (d_0) and intensity (V_0):

$$d = d_0 \sqrt[6]{\frac{V_0}{V}} \tag{1}$$

Relaxation Measurements. Proton spin−lattice longitudinal and transversal relaxation rates R_1 (= $1/T_1$) and R_2 (= $1/T_2$) were measured by inversion recovery and Carr−Purcell−Meiboom−Gill (CPMG) pulse sequences, respectively, in combination with 2D-^{1}H,^{13}C-HSQC experiment to gain resolution.[21] This was obtained by substituting the first ^{1}H 90° pulse in 2D-^{1}H,^{13}C-HSQC with a 180°-τ-90° (where τ is a variable delay) or a CPMG sequence, respectively. The 180° repetition delay in CPMG experiments was 3 ms.

Molecular Dynamics. All simulations were carried out using extensions of the GROMOS carbohydrate force field[22] within the GROMACS 4.0 program.[23] Force-field parameters for the glucose residues were adapted for building $GlcNH_2$ and GlcN-lactitol blocks. A modeled 10-mer polysaccharide filament (represented in the Table of Contents graphic) with glycosidic angles $\varphi \approx 75°$ and $\psi \approx +119°$ (where φ and ψ are defined by atoms O5−C1−O1−C4 and C1−O1−C4−C3, respectively) was used as starting structural framework in all simulations. The polymer chains were placed in a truncated

dx.doi.org/10.1021/jp4067263 | J. Phys. Chem. B 2013, 117, 13578−13587

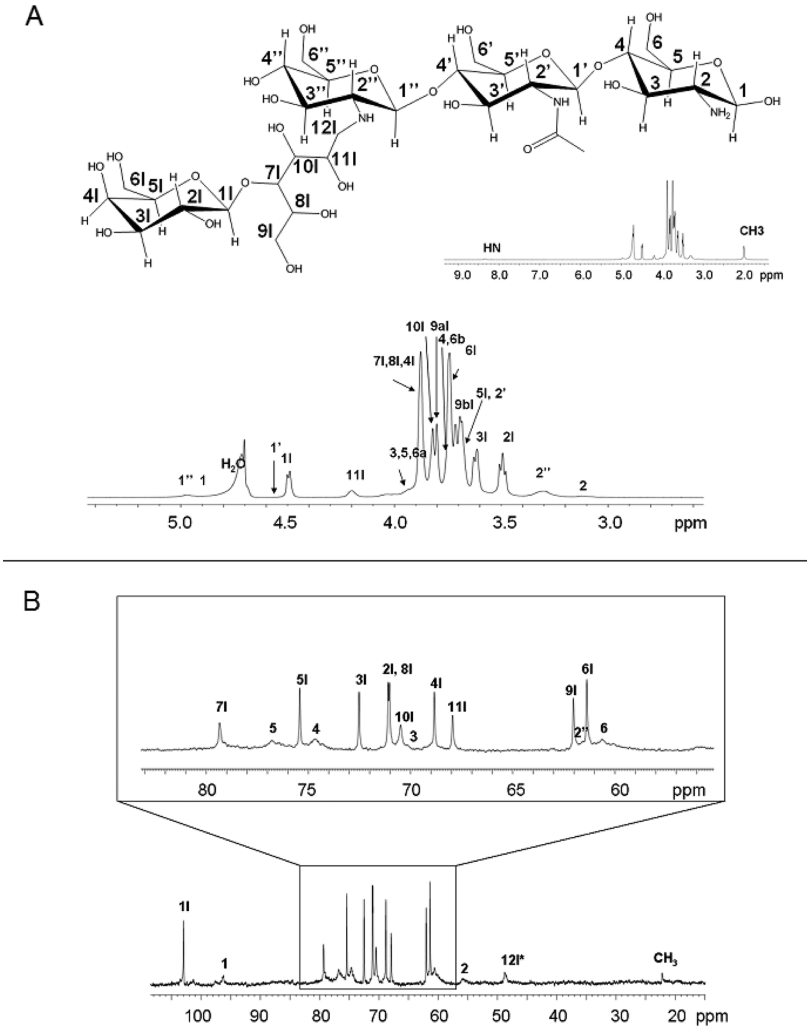

Figure 1. (A) ^{1}H and (B) ^{13}C NMR assignment for Chitlac in H_2O (10% D_2O) at 300 K, pH 4. In the atom labels, letters a and b were used to distinguish between geminal protons.

octahedral periodic simulation box, with the dimensions set to the diameter of the system (largest distance between atoms) plus 1 nm. The systems were then solvated by filling the box with SPC model water molecules.[24] Sodium and chloride ions were used to achieve the desired ionic strengths (0.25 M). Each system was energy minimized using 10 000 steps of the steepest descent method. After minimization, the solvent was equilibrated by performing 150 ps molecular dynamics simulations at 50, 100, 150, 200, 250 and 300 K, with nonhydrogen atoms positionally restrained. A total of 100 ns molecular dynamics simulations were thereafter performed in an isothermal−isobaric (NPT) ensemble using the leapfrog algorithm[25] with a 2 fs time step, therefore allowing structural flexibility of the filament along its axis. The configurations were recorded every 2 ps for analysis. During the MD simulations, at every time step, the translational and rotational motions of the center of mass were removed. The temperature was kept at 300 K by coupling the solutes and the solvent using a Nosé−Hoover[26,27] extended ensemble, with time constant for coupling of 0.5 ps. The pressure was maintained at 1 bar using the Parrinello−Rahman approach.[28] Water stretching and bending motions were constrained using the LINCS algorithm.[29] A 1.4 nm cutoff was used for the short-range electrostatics and van der Waals interactions. Long-range electrostatic contributions were treated via particle mesh Ewald method (PEM).[30,31]

RESULTS AND DISCUSSION

Solubility, Thermal Stability, and Cytotoxicity of Chitlac. The present manuscript focuses on the molecular properties of Chitlac that, at variance with its parent compound chitosan, shows a very high solubility in water independently of the pH. However, the solubility of the polysaccharide is limited when ethanol is added. As reported in Figure 1S of the Supporting Information section, at pH 4.5 chitlac is soluble up to 50% of ethanol volume fraction (ϕ_{EtOH}), while its solubility is reduced to 40% of ϕ_{EtOH} when the pH is increased to 7.4. Although a more detailed thermal analysis of the polysaccharide is deferred to further work, preliminary DSC and TGA measurements showed that degradation occurs at ∼250 °C (Figure 2S in Supporting Information). Chitac has been proven to be noncytotoxic toward cell lines[15] and primary cultures[6,14,18] and did not show bacteriostatic effect toward *S. aureus* (Figure 3S in Supporting Information).

^{1}H and ^{13}C NMR Assignment and Apparent pK_a Values for Chitlac. Chitlac has been studied by means of ^{1}H and ^{13}C NMR, and a complete assignment of the peaks has been attained for both the backbone and the side chains

dx.doi.org/10.1021/jp4067263 | J. Phys. Chem. B 2013, 117, 13578−13587

(Figure 1). Recognition of the signals pertaining to the backbone was guided by the NMR analyses performed on chitosan (not reported), whose signals are sharper in the absence of substitution. Indeed, this effect depends on the degree of lactosylation of the chitosan sample, with the Chitlac sample at the highest content of lactitol side chains (58%) showing the broader NMR signals from the backbone. Shorter transversal relaxation time of the polysaccharide chain (causing broadening) may be simply due to the increase in molecular weight as a consequence of the derivatization, leading to a reduced overall tumbling of the molecule. The degree of acetylation and lactosylation can be readily calculated from the analysis of 1D ^{1}H NMR spectra recorded at 343 K, which avoids overlapping between the residual water signal and the anomeric protons of the rings. (See Figure 4S in the Supporting Information.) However, the degree of lactosylation and acetylation can also be determined at lower temperature by using H_2 protons of the sugar rings as shown in the bottom part of Figure 2. The figure also reports 1D spectra of Chitlac upon increasing lactosylation degree.

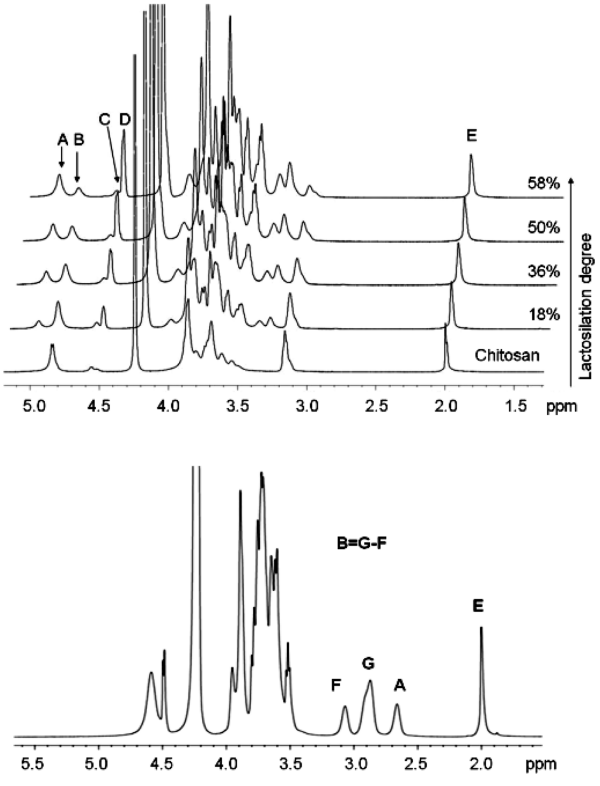

Figure 2. 1D ^{1}H NMR spectra of CHITLAC with increasing degrees of lactosylation (top) at 343 K, pH 4. (bottom) Relevant peaks for the estimation of the lactosylation degree in cases where anomeric protons are not clearly visible (T = 343 K, pH 7). Acetylation α (= 100(E/3)/(A + B + E/3)) and lactosilation β (= A(100 − α)/(A + B)) can be estimated by substituting the integrals of corresponding label in the formulas. Note that labels refer to different signals in the two panels. In the top panel, A−C indicate the anomeric protons of secondary amine, primary amine, and acetylated backbone rings, respectively. D is the anomeric proton of the residual galactose in the lactitol side chain, while E is the methyl group of *N*-acetylglucosamine residues. In the bottom panel, A is the H_2 proton of the ring bearing the secondary amine, B is the H_2 of the ring bearing the primary amine (after subtraction of the overlapped H_{12} from integral G), and F is the integral of the equally intense geminal H_{12} proton.

From a series of NMR spectra recorded at different pH values (Figure 3), it is possible to determine the "stoichio-

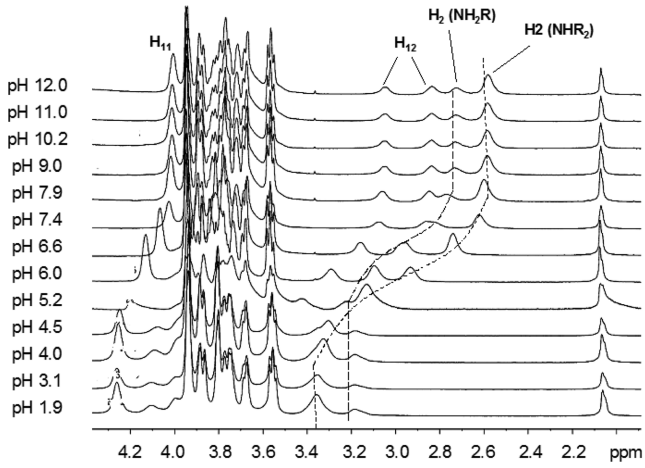

Figure 3. ^{1}H NMR spectra of Chitlac in water (10% D_2O) at the concentration of 10 mg/mL in a range of pH between 1.9 and 12.0. T = 343 K.

metric" value of the "apparent pK_a" $[(pK_a)]^{app}_{(\alpha=0.5)}$ for each of the two amino groups. This apparent value, determined as described in the Supporting Information section, is the value of pH at which the stoichiometric concentrations of the charged and of the uncharged species (i.e., 50% of dissociation for that particular group, corresponding to α = 0.5) are equal. It is not a thermodynamic value (e.g., a p$K°$ corresponding to a $\Delta G°$) both for its purely stoichiometric origin and because it conceptually refers, for each of the two groups, to two specific values (albeit very close) of overall charge density of the chain. The acid/base characteristics of polyelectrolytes with even only one type of such groups (i.e., one value of p$K°$, namely, polymonoprotic acids) can be described only by an α-dependent apparent value of pK_a: $pK^{app}(\alpha) = pK° + ((\Delta G^{el}(\alpha))/(2.303RT))$, where p$K°$ and $\Delta G^{el}(\alpha)$ are the value of the dissociation constant of the first acid/base group in the uncharged chain and the excess polyelectrolytic free energy at the degree of dissociation α, respectively.[32] It should also be recalled that $\Delta G^{el}(\alpha)$ is strongly dependent on the ionic strength of the system as well as on temperature. Similar equations hold for more complex systems, like polydiprotic acids.[33,34] The Figure shows how the chemical shift of H_2 protons of the chitosan rings (located nearby the amino groups) is highly sensitive to the protonation equilibrium and can therefore be used to determine $[(pK_a)]^{app}_{(\alpha=0.5)}$ values (see Figure 5S in Supporting Information section). The analyses of the experimental results indicated that the $[(pK_a)]^{app}_{(\alpha=0.5)}$ values are 6.69 and 5.87 for the primary and secondary amines, respectively.

The value of $[(pK_a)]^{app}_{(\alpha=0.5)}$ for the secondary amines was confirmed using the chemical shift of geminal H_{12} and H_{11} protons obtaining similar values (5.91, 5.79, and 5.93, respectively). 2D NOESY was used to resolve the overlap of H_{12} with H_2 protons at low pH values and exactly determine its chemical shift. (Figure 4).

The experimental data on the $[(pK_a)]^{app}_{(\alpha=0.5)}$ values of the primary and secondary amines are in good agreement with those reported in the literature for similar chitosan derivatives,[35] confirming the validity of the determinations. As pointed out by Tømmeraas and coworkers,[35] the low

dx.doi.org/10.1021/jp4067263 | J. Phys. Chem. B 2013, 117, 13578−13587

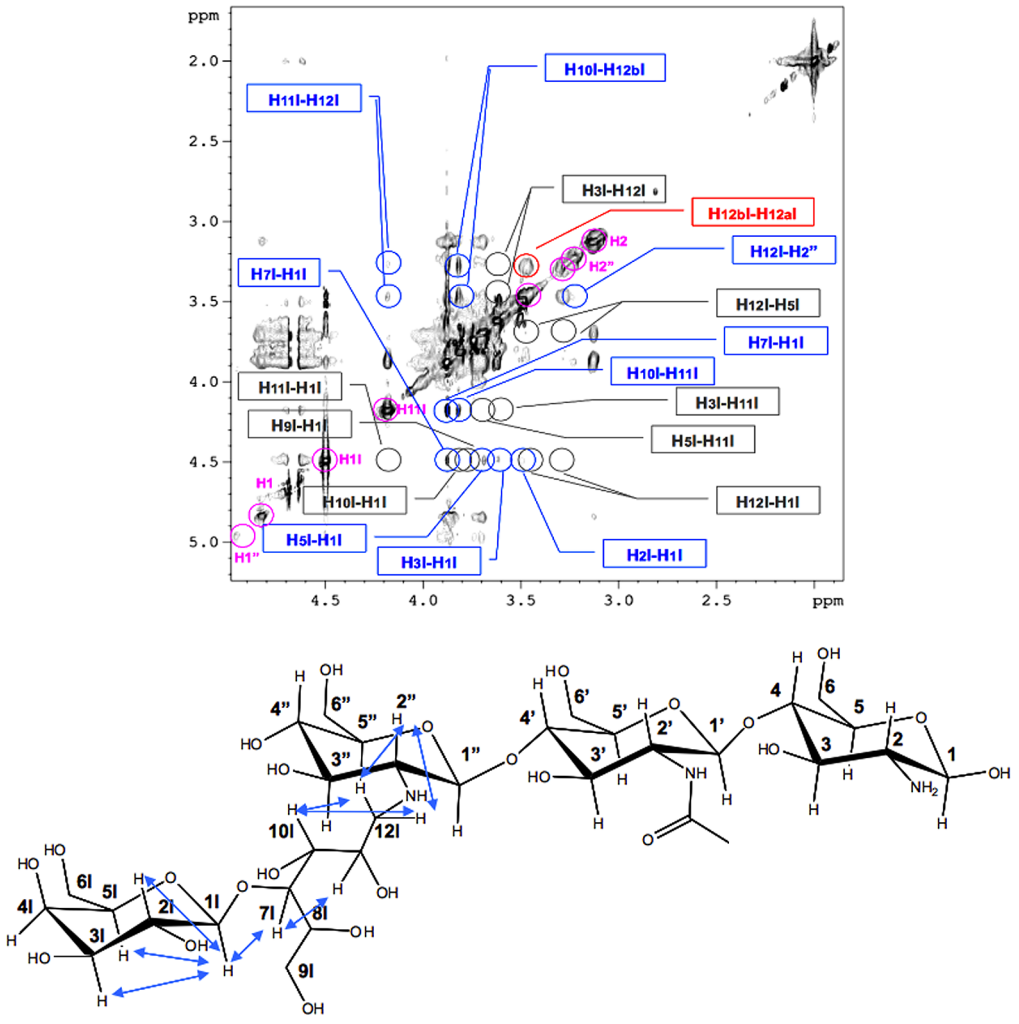

Figure 4. (top) ^{1}H,^{1}H-2D NOESY spectrum of Chitlac in D_2O (pD 4, T = 300K). Unambiguous meaningful NOEs are shown in blue. Empty regions indicating the absence of NOE between two protons are shown in dark gray; the NOE peak used for distance calibration connecting H_{12} geminal protons (distinguished with letters a and b) is shown in red. Other diagonal peaks are shown in magenta. (bottom) NOE network regarding the lactitol moiety is shown on the Chitlac molecular structure.

$[(pK_a)]^{app}_{(\alpha=0.5)}$ value of the secondary amine with respect to the primary one points to a possible involvement of the lactitol side chain in an interaction (likely hydrogen bonding) with the chitosan backbone. We will discuss this issue further in the text.

Conformational Properties of the Lactitol Side Chain. To shed light on the side-chain conformation, we used NMR and molecular dynamics. Because of the large size of the polymer, NOE transfer is very effective, and it can be used to determine the average conformation. Mixing times have to be kept short to avoid spin diffusion effects (typically 70 ms).

Figure 4 shows the NOESY spectrum of Chitlac, indicating the unambiguously assigned significant NOEs. Despite the strong overlap and the large number of signals, some well-resolved protons (whose NOESY cross peaks are shown in blue in Figure 4) help in defining the conformation of the lactitol in the polymer. The experiment was performed on chitosan and on Chitlac with four increasing degrees of lactosylation to monitor a possible dependence of the conformational properties on the lactosylation degree. However, the pattern of interproton NOEs remains very similar in all samples (not reported), at least for the isolated and unambiguously assigned NOEs.

Interproton distances were calculated by means of eq 1 from NOE cross peak intensities using the Chitlac sample with the largest degree of lactosylation (58%) to have the best signal-to-noise ratio.

Table 1 reports the distances relating atoms of the lactitol side chain, among themselves and with $H_{2''}$ atom on the main polymeric chain.

As shown in Figure 4, NOEs $H_{1l}\rightarrow H_{3l}$ and $H_{1l}\rightarrow H_{5l}$ demonstrate than the ring in the lactitol moiety adopts a chair conformation with the larger substituent in equatorial position. NOEs $H_{1l}\rightarrow H_{7l}$, $H_{7l}\rightarrow H_{11l}$, $H_{10l}\rightarrow H_{12l}$, $H_{10l}\rightarrow H_{11l}$, and $H_{11l}\rightarrow H_{12l}$ define the conformation of the remaining part of the lactitol chain, with H_{7l} sensing H_{1l} near, H_{11l} sensing H_{7l} nearer than H_{12l}, and H_{10l} sensing H_{12l} nearer than H_{1l}. It is pointed out that even though Figure 4 shows a side-chain conformation compatible to the experimental data, relaxation measurements revealed a substantial degree of motion for the lactitol moiety and the structure derived from NOEs is considered to be only the average of many possible others.

Finally, the presence of NOEs between $H_{2''}$ and H_{12l} (not quantifiable for strong overlap but stronger than the NOE with $H_{3''}$ or $H_{5''}$) seems to suggest that the orientation of the full lactitol is pointing away from the Chitosan backbone. Very

dx.doi.org/10.1021/jp4067263 | J. Phys. Chem. B 2013, 117, 13578−13587

Table 1. Interproton Distances Derived from NOESY Spectrum of Chitlac (at 60% Lactosylation Degree)[a]

proton atoms	distance (Å)
H_{11l}–$H_{12'l}$	2.5*
H_{11l}–H_{12l}	2.36
$H_{12'l}$–H_{10l}	2.16
H_{12l}–H_{10l}	2.2*
H_{11l}–H_{10l}	2.3*
H_{1l}–H_{5l}	2.36
H_{1l}–H_{3l}	2.61
H_{1l}–H_{2l}	2.87
H_{7l}–H_{11l}	2.35
$H_{2''}$–H_{12l} (*)	2.36
$H_{2''}$–H_{11l} (*)	2.51

[a]* indicates larger experimental error.

weak long-range NOE peaks can be found in NOESY spectra ($H_{2''}$→H_{7l}; $H_{2''}$→H_{6l}) even with short mixing times (70 ms), but they were not interpreted as structural constraints because relaxation measurements demonstrated high flexibility of the lactitol moiety. (The sixth power dependency of the interproton distance in the NOE effect makes conformations involving close contact visible even if poorly populated.)

The absence of selected interproton NOEs (shown in dark gray in Figure 4) is also informative in excluding other possible long-range interactions within the lactitol moiety. These data, however, cannot rule out the presence of hydrogen bonds between the lactitol side chain and the chitosan backbone, which might explain the low $[(pK_a)]^{app}_{(\alpha=0.5)}$ value of secondary amines, as suggested by Tømmeraas and coworkers.[35] In particular, given the lower mobility observed for lactitol protons close to the chitosan backbone (see relaxation data in Figure 5), NMR data cannot exclude the presence of a hydrogen bond between the secondary amine and the hydroxyl in position 11 on the side chain. Indeed, molecular dynamics analyses performed in the present work confirmed the presence of hydrogen bonds NH···O_{10l} and NH···O_{11l} between the lactitol chain and polysaccharide backbone. These two H bonds seem to be complementary and, according to time trajectories shown in Figure 6 of the Supporting Information, are present for ∼27% of total simulation time.

Dynamics of the Lactitol Side Chain As Derived by NMR Relaxation. To get insight into the dynamics of the polymer, we measured R_1 and R_2 relaxation rates. Before going into the details of the calculation, it is worth noticing that there is a significant difference in R_2 values when comparing the chitosan backbone and the lactitol chain. This is evident when registering the ^{1}H-,^{13}C-HSQC spectrum of the polymer, where only the signals from the lactitol moiety are clearly visible despite their lower amount (the lactosylation degree is only 18%) with respect to those of the backbone. This is due to the shorter lifetime of the latter, most likely caused by slow molecular tumbling. Apparently, the lactitol moiety undergoes fast motion and it is unlikely to strongly interact with the chitosan main chain. This also explains why such a large molecule gives quite good spectra and demonstrates that the interactions of the very flexible side chains are short-lived and unable to stabilize a well-defined conformation.

A more quantitative analysis can be obtained by calculating the reorientational correlation time for each proton in the lactitol chain. This measurement allows us to localize the region of the molecule undergoing fast motion and detect how dynamics is affected by the lactosylation degree. The relaxation rate of the molecule depends on local motions, which are described by the correlation time, τ_c, and interproton distances. In the present case, interproton distances are not directly measurable due to the flexibility of the lactitol side chain. However, the dependence on this parameter can be ignored using the ratio between R_1 and R_2 according to the following eq 2:[36]

$$\frac{R_1}{R_2} = \frac{\frac{6\tau_c}{(1+\omega_H^2\tau_c^2)} + \frac{24\tau_c}{(1+4\omega_H^2\tau_c^2)}}{\frac{15\tau_c}{(1+\omega_H^2\tau_c^2)} + \frac{6\tau_c}{(1+4\omega_H^2\tau_c^2)} + 9\tau_c} \quad (2)$$

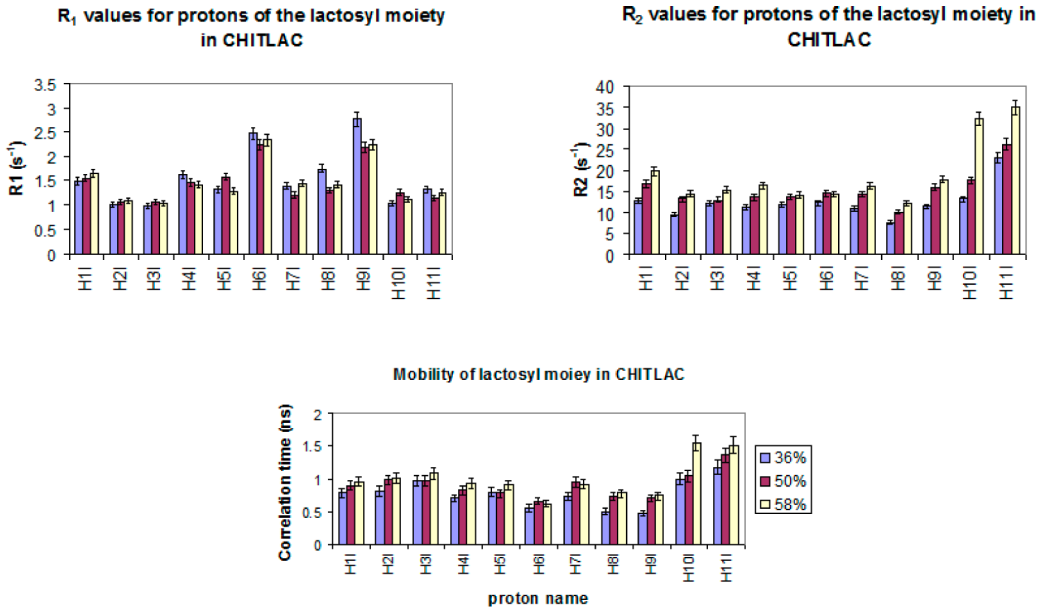

Figure 5. Relaxation R_1 and R_2 and motional correlation time for protons in the lactosyl moiety of Chitlac at different lactosylation degrees, namely, 36% (blue), 50% (red), and 58% (yellow).

dx.doi.org/10.1021/jp4067263 | J. Phys. Chem. B 2013, 117, 13578−13587

where ω_H is the proton Larmor frequency and τ_c is the correlation time modulating the dipolar interaction.

Equation 2 is valid in the absence of chemical exchange and in cases where the relaxation mechanism is purely dipolar. Even though spin rotational contribution can be present in our system, they are unlikely to dominate over dipolar mechanism.

Because of extended overlap in the ^{1}H NMR spectrum, the relaxation rates R_1 and R_2 of the individual protons were determined using a combination of inversion recovery (or CPMG) pulse sequence with a 2D NMR experiment (in the present case ^{1}H−^{13}C HSQC).[21] In this way, it was possible to measure relaxation parameters for all unexchangeable protons in the lactitol moiety (mostly overlapped in the 1D version), with an exception made for H_{12l}, whose R_2 was too fast to generate a measurable signal in the 2D spectra.

The results are shown in Figure 5. For all lactosylation degrees there is an increase in R_2 values as we move nearer to the chitosan chain, most likely indicating a more restricted motion close to the linking site.

Data reported in Figure 5 indicate that the motion of the Chitlac molecule slows down upon increasing the lactosylation degree. This effect is observed in almost all protons but it is more evident for H_{10l} and H_{11l}, which are more restrained in the local movement and might provide a good probe for the dynamics of the backbone. The slowing of the motion can be partially explained by the increase in the molecular weight due to lactitol substitution but could also indicate stronger interaction with the solvent.

As far as the lactitol chain is concerned, relaxation data clearly indicate enhanced mobility for this part of the molecule with respect to the polymer backbone. The correlation times of the residual galactose ring and those of the linker chain-element (protons H_{7l}−H_{9l} of glucitol) are significantly lower than that of H_{11l}, which is the best probe available for the chitosan backbone. The large broadening of the chitosan signals prevents the quantitative measurement of mobility but indicates motions slower than that of H_{11l}. Finally, the low correlation time of H_{6l} reflects the fast dynamics of the methylene protons of the galactose ring.

As previously stated, besides the fast motion of the lactitol chains, experimental data do not show significant shift of NMR signals for different degrees of substitution. All of these observations tend to exclude a polymeric conformational change induced by steric hindrance among lactitol moieties that could produce some degree of ordering of the side chains.

Comparison of NMR-Derived Interatomic Distances with Molecular Dynamics Calculations. For the study of interatomic distances and dihedral angles of the side chain, we used a combined approach that complemented NMR measurements with MD simulations of chitosan decamers at different degrees of lactitol substitution.

Figure 4 shows all relevant atoms of the side chain and of the corresponding chitosan repeating unit. The present MD analysis finds that only dihedral angles A1, A2, and A3 (defined by atoms $C_{2''}$−N−C_{12l}−C_{11l}; N−C_{12l}−C_{11l}−C_{10l}; and C_{12l}−C_{11l}−C_{10l}−C_{7l}, respectively) could be correlated with the conformational preferences of the side chain. (See Figure 6.)

Table 2 includes four relevant interatomic distances, as identified by the NOE experiments, along with the corresponding mean values obtained in the MD calculations. As previously noted, these NMR data correspond to Chitlac samples with lactosylation degree close to 60%, which minimized experimental error. The MD data correspond to the lactitol side chain attached to the sixth unit of chitosan decamers at 60% lactosylation degree. Out of these four distances, the first and last correspond to the separation between atoms of the main chitosan chain and atoms of the side chain.

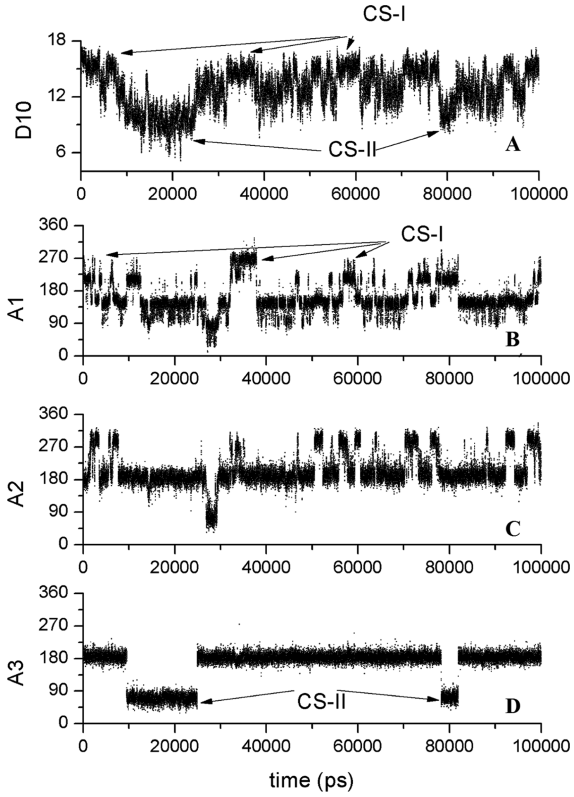

Figure 6. (A) Time dependence of the interatomic distance D10 (C4l−N5)(in Å) and time trajectories of the dihedral angles A1 (B), A2 (C), and A3 (D) of the first lactitol unit. Approximate time intervals corresponding to Conformational switches CS-I and CS-II have been identified.

The table also includes the standard deviation and minimum and maximum values of the corresponding distance obtained from the 100 ns MD simulation.

It is readily seen that these calculated distances are short enough to be seen by NMR-NOE experiments and that there is a good agreement between experimental and calculated values, considering the unified atom approximation used in the present simulations and the experimental error.

It is important to stress that these distances are very similar for all lactitol side chains, regardless of their position along the decamer, a characteristic that is fully shared by the NMR data. As an example, Table 3 shows the MD calculated $C_{2''}$−C_{12l} distance for all six lactitol side chains of the Chitlac decamer at 60% lactosylation. The NOE experimentally determined distance is also included for comparison.

To gain some understanding of the lactitol side-chain conformation, it is important to determine the MD calculated time trajectory of the distance between atoms on the main chain and those at the far end of the lactitol side chain. Figure 6a shows the time variation of the distance D10 (defined as the distance between the furthest C on the lactitol side chain (C_{4l}) attached to the sixth decamer unit and the N atom of the previous backbone monomer (in this case of the fifth monomer, N_5)). Besides its fast fluctuations, two zones of different mean values can be readily identified: an extended conformation (D10 ≈ 15 Å) labeled Conformational Switch I

dx.doi.org/10.1021/jp4067263 | J. Phys. Chem. B 2013, 117, 13578−13587

Table 2. Average Values of NOE and MD Distances (in Å) Involving Atoms of the Lactitol Side Chain[a]

			MD simulation (Å)			
distance label	end atoms	NOE-NMR	mean	S. D.	min	max
D12	$C_{2''}$–C_{12l} ($H_{2''}$–H_{12l})	2.36	2.54	0.04	2.28	2.67
D13	C_{10l}–C_{12l} (H_{10l}–H_{12l})	2.16	2.52	0.05	2.27	2.72
D14	C_{10l}–C_{11l} (H_{10l}–H_{11l})	2.32	1.53	0.01	1.52	1.54
D15	$C_{2''}$–C_{11l} ($H_{2''}$–H_{11l})	2.51	3.73	0.15	2.95	4.02

[a]Standard deviations and minimum and maximum calculated values are also included.

Table 3. Experimental (NOE-NMR) ($H_{2''}$–H_{12l}) and Calculated (MD) ($C_{2''}$–C_{12l}) Distance for the Six Lactitol Side Chains of the Chitlac Decamer at 60% Lactosylation

NOE-NMR	MD		
$H_{2''}$–H_{12l} distance (Å)	lactitol unit	$C_{2''}$–C_{12l} distance (Å)	SD (Å)
	Chil2	2.49	0.05
	Chil4	2.54	0.04
	Chil6	2.54	0.04
	Chil7	2.54	0.04
	Chil8	2.54	0.04
	Chil10	2.50	0.05
2.36	mean	2.53	

(CS-I) in Figure 6a and a second region where these end atoms are closer together (~9 Å), identified as Conformational Switch II (CS-II).

To understand the origin of these distance regions, Figure 6 reports the time variation of the dihedral angles A1, A2, and A3 (of the first lactitol unit), which are the only ones that seem to correlate with the changes in distance D10. The trajectory of angle A3 occurs in two well-defined and rather stable zones, one around 180° and the other around 60°. This latter zone correlates very well with zones of shorter values of the D10 distance, which were indicated as Conformational Switch II, while Conformational Switch I seems to correlate well with changes of the dihedral angle A1. The latter angle seems to be, together with A2, an important source of D10 fast variations.

Conformational switches CS-I and CS-II have therefore been identified as the two more relevant orientation of the lactitol side chain (with respect the main chitosan chain): a rather extended conformation pointing away from the main chain (CS-I) and a folded conformation, CS-II, where the lactose monomer on the side chain bends toward the main chain becoming almost parallel to it, as shown in the two snapshots of Figure 7, taken from the decamer trajectory approximately at times 3.6 and 16.1 ns, respectively. Similar results are obtained for lactitol side chains at different lactosylation degrees. Interestingly, CS-II is consistent with a short $H_{11l}\cdots H_{2l}$ interproton distance (~1.5 Å) which should otherwise be much larger (more than ~4 Å in the extended conformation). Indeed, an unambiguous NOESY cross peak between the signals of these two protons is observed. Its volume was not translated into distance as its intensity is probably scaled by the limited fraction of lactitol in the CS-II conformation; however, its presence qualitatively supports the MD calculations. These results and the presence of the two hydrogen bonds between the lactitol side chain and the polysaccharide backbone support the hypothesis that the lactitol is always pointing away from the main chain, adopting folded conformations only through a bending of the second lactitol unit, which becomes parallel to the CS main chain (Conformational Switch II).

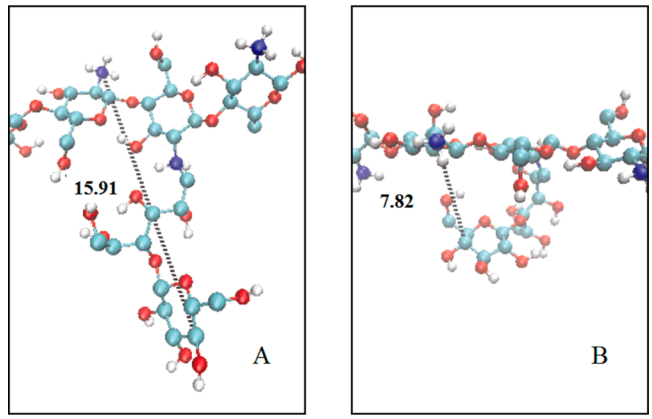

Figure 7. MD snapshots showing the orientation of the lactitol side attached to the sixth unit of Chitlac decamer in the regions of Conformational Switches I (A) and II (B). The distance D10 (in Å) between atom C4l at the far end of lactitol and the N5 atom of the preceding chitosan repeating unit is quoted in each case.

Another feature to support this thesis is the calculated solvent-accessible surface area (SASA) of the lactitol side chain to the solvent molecules, which could detect differences in the degree of solvation in the two characteristic conformations of the side chain (CS-I and CS-II). SASA calculations are illustrated in Figure 8, which readily shows that in both conformations the side chain is well inserted into the solvent, always adopting hydrophilic conformations.

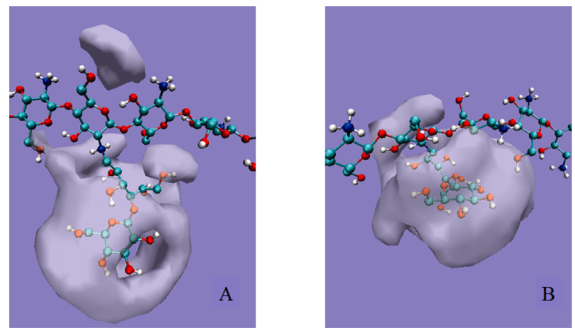

Figure 8. Solvent-accessible surface area (SASA) of the lactitol side chain in CS-I (A, extended conformation) and CS-II (B, folded conformation).

The qualitative picture given by Figure 8 is consistent with the time dependence of the solvent-accessible surface area of the lactitol side chain of Figure 7 of the Supporting Information, which shows that SASA fluctuates around a mean value of ~3.8 nm^2, with zones of slightly smaller area (10% smaller), indicating that the side chain is always well-solvated. The regions of smaller SASA are in the time interval

dx.doi.org/10.1021/jp4067263 | J. Phys. Chem. B 2013, 117, 13578–13587

12−24 ns, which correlates quite well with a similar region of Figure 6 corresponding to CSII, indicating that this small decrease in SASA could be attributed to the bending of the lactitol side chain.

CONCLUSIONS

The conformational properties of Chitlac, a modified chitosan with bioactive features toward chondrocytes and osteoblasts,[6,14,15,18] has been studied regarding its lactitol side chains at different lactosylation degrees. In particular, NOE-NMR and MD-derived side-chain interatomic distances showed a good agreement within the experimental error and the unified atom approximation used in these simulations. Both techniques also point to a higher flexibility and dynamics of the lactitol side chain when compared with the chitosan backbone. In addition, the lactitol side chains seem to adopt two distinct conformational orientations with respect to the polysaccharide chain: a folded conformation, with the residual galactose ring of the lactitol moiety parallel to the main chain (CS-II), and an extended conformation, pointing away from the chitosan chain (CS-I). It is also found that the average orientation of the lactitol moiety does not depend on the lactosylation degree. Both NMR experimental data and MD calculations rule out the hypothesis of a conformational change (or ordering of the side chains) due to increased lactosylation degree. Moreover, in all conformations, the side chains of Chitlac are well-immersed in the solvent, showing a good degree of solvation, without forming any stable interactions with the main chain. The absence of strong interactions involving the terminal galactose and its exposition to the solvent may at least partially account for the overall biocompatibility of the polymer. An extended analysis of the conformational properties of the whole modified polysaccharides, which includes the chitosan backbone, will be targeted in a forthcoming manuscript.

ASSOCIATED CONTENT

Supporting Information

Composition of Chitlac samples. Transmittance dependence of Chitlac solutions on ethanol volume fractions in water/ethanol mixtures. DSC and TGA of Chitlac. *S. aureus* growth inhibition in the presence of Chitlac. Temperature dependence of ^{1}H NMR spectra of Chitlac. pK_a dermination based on pH dependence of backbone H_2 chemical shifts. MD-derived time trajectories indicating the existence of H-bonds NH..O_{10l} and NH..O_{11l}. Solvent-accessible surface area of the lactitol side chains in Chitlac. This material is available free of charge via the Internet at http://pubs.acs.org.

AUTHOR INFORMATION

Corresponding Author

*E-mail: n.d'amelio@ucl.ac.uk.

Present Addresses

[#]Department of Chemistry and Institute of Structural and Molecular Biology, University College London, London WC1E 6BT, United Kingdom. Tel: (+44) 020 76793215.

[▽]Novartis Vaccines & Diagnostics, Technology Development, via Fiorentina 1, 53100 Siena, Italy.

Notes

The authors declare no competing financial interest.

ACKNOWLEDGMENTS

We thank Chiara Vatta for skillful assistance in the experimental part and Michela Cok (University of Trieste) for DSC and TGA measurements. This work has been developed under the auspices of the Universidad Nacional de San Luis (UNSL)-Università di Trieste bilateral agreement. The San Luis group also acknowledges the support of CONICET (Argentina) through project PID 6296 and UNSL through project P32-8402. J.B. is a member of Carrera del Investigador, CONICET. J.B. acknowledges the generous support of the Università di Trieste for his visits to the Trieste group.

ABBREVIATIONS

CS, conformational switch; PEM, particle mesh Ewald method; COSY, correlation spectroscopy; CPMG, Carr−Purcell−Meiboom−Gill pulse sequence; DSC, differential scanning calorimetry; HEK293, human embryonic kidney 293 cell lines; HSQC, heteronuclear single quantum coherence; LINCS, linear constraint solver for molecular simulations with bond constraints; NOESY, nuclear Overhauser effect spectroscopy; SASA, solvent-accessible surface area; TGA, thermogravimetric analysis; TOCSY, total correlation spectroscopy

REFERENCES

(1) Strand, S. P.; Tømmeraas, K.; Vårum, K. M.; Østgaard, K. Electrophoretic Light Scattering Studies of Chitosans with Different Degrees of N-Acetylation. *Biomacromolecules* **2001**, *2*, 1310−1314.

(2) Di Martino, A.; Sittinger, M.; Risbud, M. V. Chitosan: A Versatile Biopolymer for Orthopaedic Tissue-Engineering. *Biomaterials* **2005**, *26*, 5983−5990.

(3) Francis Suh, J. K; Matthew, H. W. T. Application of Chitosan-Based Polysaccharide Biomaterials in Cartilage Tissue Engineering: A Review. *Biomaterials* **2000**, *21*, 2589−2598.

(4) Strand, S. P.; Issa, M. M.; Christensen, B. E.; Vårum, K. M.; Artursson, P. Tailoring of Chitosans for Gene Delivery: Novel Self-Branched Glycosylated Chitosan Oligomers with Improved Functional Properties. *Biomacromolecules* **2008**, *9*, 3268−3276.

(5) Yalpani, M.; Hall, L. D.; Tung, M. A.; Brooks, D. E. Unusual Rheology of a Branched, Water-Soluble Chitosan Derivative. *Nature* **1983**, *302*, 812−814.

(6) Marcon, P.; Marsich, E.; Vetere, A.; Mozetic, P.; Campa, C.; Donati, I.; Vittur, F.; Gamini, A.; Paoletti, S. The Role of Galectin-1 in the Interaction Between Chondrocytes and a Lactose-Modified Chitosan. *Biomaterials* **2005**, *26*, 4975−4984.

(7) Barondes, S. H.; Cooper, D. N.; Gitt, M. A.; Leffler, H. Galectins. Structure and Function of a Large Family of Animal Lectins. *J. Biol. Chem.* **1994**, *269*, 20807−20810.

(8) Kopitz, J.; von Reitzenstein, C.; Burchert, M.; Cantz, M.; Gabius, H.-J. Galectin-1 Is a Major Receptor for Ganglioside GM1, a Product of the Growth-controlling Activity of a Cell Surface Ganglioside Sialidase, on Human Neuroblastoma Cells in Culture. *J. Biol. Chem.* **1998**, *273*, 11205−11211.

(9) Gu, M.; Wang, W.; Song, W. K.; Cooper, D. N.; Kaufman, S. J. Selective Modulation of the Interaction of Alpha 7 Beta 1 Integrin with Fibronectin and Laminin by L-14 Lectin During Skeletal Muscle Differentiation. *J. Cell Sci.* **1994**, *107*, 175−181.

(10) Hernandez, J. D; Baum, L. G. Ah, Sweet Mystery of Death! Galectins and Control of Cell Fate. *Glycobiology* **2002**, *12*, 127R−136R.

(11) Maeda, N.; Kawada, N.; Seki, S.; Arakawa, T.; Ikeda, K.; Iwao, H.; Okuyama, H.; Hirabayashi, J.; Kasai, K. i.; Yoshizato, K. Stimulation of Proliferation of Rat Hepatic Stellate Cells by Galectin-1 and Galectin-3 through Different Intracellular Signaling Pathways. *J. Biol. Chem.* **2003**, *278*, 18938−18944.

(12) Ozeki, Y.; Matsui, T.; Yamamoto, Y.; Funahashi, M.; Hamako, J.; Titani, K. Tissue Fibronectin is an Endogenous Ligand for Galectin-1. *Glycobiology* **1995**, *5*, 255−261.
(13) Hirabayashi, J.; Hashidate, T.; Arata, Y.; Nishi, N.; Nakamura, T.; Hirashima, M.; Urashima, T.; Oka, T.; Futai, M.; Muller, W. E.; et al. Oligosaccharide Specificity of Galectins: A Search by Frontal Affinity Chromatography. *Biochim. Biophys. Acta* **2002**, *1572*, 232−254.
(14) Donati, I.; Stredanska, S.; Silvestrini, G.; Vetere, A.; Marcon, P.; Marsich, E.; Mozetic, P.; Gamini, A.; Paoletti, S.; Vittur, F. The Aggregation of Pig Articular Chondrocyte and Synthesis of Extracellular Matrix by a Lactose-Modified Chitosan. *Biomaterials* **2005**, *26*, 987−998.
(15) Travan, A.; Marsich, E.; Donati, I.; Foulc, M. P.; Moritz, N.; Aro, H. T.; Paoletti, S. Polysaccharide-Coated Thermosets for Orthopedic Applications: From Material Characteization to In Vivo Tests. *Biomacromolecules* **2012**, *13*, 1564−1572.
(16) Donati, I.; Borgogna, M.; Turello, E.; Cesàro, A.; Paoletti, S. Tuning Supramolecular Structuring at the Nanoscale Level: Non-stoichiometric Soluble Complexes in Dilute Mixed Solutions of Alginate and Lactose-Modified Chitosan (Chitlac). *Biomacromolecules* **2007**, *8*, 1471−1479.
(17) Donati, I.; Haug, I. J.; Scarpa, T.; Borgogna, M.; Draget, K. I.; Skjåk-Bræk, G.; Paoletti, S. Synergistic Effects in Semidilute Mixed Solutions of Alginate and Lactose-Modified Chitosan (Chitlac). *Biomacromolecules* **2007**, *8*, 962.
(18) Marsich, E.; Borgogna, M.; Donati, I.; Mozetic, P.; Strand, B. L.; Gomez-Salvador, S.; Vittur, F.; Paoletti, S. Alginate/Lactose-Modified Chitosan Hydrogels: A Bioactive Biomaterial for Chondrocyte Encapsulation. *J. Biomed. Mater. Res.* **2008**, *84A*, 364−376.
(19) DeMarco, M. L; Woods, R. J. Structural Glycobiology: A Game of Snakes and Ladders. *Glycobiology* **2008**, *18*, 426−440.
(20) Almond, A.; DeAngelis, P. L.; Blundell, C. D. Hyaluronan: The Local Solution Conformation Determined by NMR and Computer Modeling is Close to a Contracted Left-handed 4-Fold Helix. *J. Mol. Biol.* **2006**, *358*, 1256−1269.
(21) D'Amelio, N.; Gaggelli, E.; Gaggelli, N.; Molteni, E.; Baratto, M. C.; Valensin, G.; Jezowska-Bojczuk, M.; Szczepanik, W. NMR and EPR Structural Delineation of Copper(II) Complexes Formed by Kanamycin A in Water. *Dalton Trans.* **2004**, 363−368.
(22) Lins, R. D; Hunenberger, P. H. A New GROMOS Force Field for Hexopyranose-Based Carbohydrates. *J. Comput. Chem.* **2005**, *26*, 1400−1412.
(23) Van Der Spoel, D.; Lindahl, E.; Hess, B.; Groenhof, G.; Mark, A. E.; Berendsen, H. J. GROMACS: Fast, Flexible, and Free. *J. Comput. Chem.* **2005**, *26*, 1701−1718.
(24) Berendsen, H. J. C.; Postma, J. P. M.; van Gunsteren, W. F.; Hermans, J. Interaction Models for Water in Relation to Protein Hydration.In *Intermolecular Forces*; Pullman, B., Ed.; D. Reidel Publishing Company; Dordrecht, The Netherlands, 1981; pp 331−342.
(25) Hockney, R. W.; Goel, S. P.; Eastwood, J. W. Quiet High-Resolution Computer Models of a Plasma. *J. Comput. Phys.* **1974**, *14*, 148−158.
(26) Hoover, W. G. Canonical Dynamics: Equilibrium Phase-Space Distributions. *Phys. Rev. A* **1985**, *31*, 1695−1697.
(27) Nosé, S. A Molecular Dynamics Method for Simulations in the Canonical Ensemble. *Mol. Phys.* **1984**, *52*, 255−268.
(28) Parrinello, M.; Rahman, A. Polymorphic Transitions in Single Crystals: A New Molecular Dynamics Method. *J. Appl. Phys.* **1981**, *52*, 7182−7190.
(29) Hess, B.; Bekker, H.; Berendsen, H. J. C.; Fraaije, J. G. E. M. LINCS: A Linear Constraint Solver for Molecular Simulations. *J. Comput. Chem.* **1997**, *18*, 1463−1472.
(30) Darden, T.; York, D.; Pedersen, L. Particle Mesh Ewald: An N·log(N) method for Ewald sums in large systems. *J. Chem. Phys.* **1993**, *98*, 10089−10092.
(31) Essmann, U.; Perera, L.; Berkowitz, M. L.; Darden, T.; Lee, H.; Pedersen, L. G. A Smooth Particle Mesh Ewald Method. *J. Chem. Phys.* **1995**, *103*, 8577−8593.
(32) Tanford, C. *Physical Chemistry of Macromolecules*; John Wiley & Sons, Inc.: New York, 1961.
(33) Dubin, P.; Strauss, U. P. Hydrophobic Hypercoiling in Copolymers of Maleic Acid and Alkyl Vinyl Ethers. *J. Phys. Chem.* **1967**, *71*, 2757−2759.
(34) Dubin, P. L.; Strauss, U. P. Hydrophobic Bonding in Alternating Copolymers of Maleic Acid and Alkyl Vinyl Ethers. *J. Phys. Chem.* **1970**, *74*, 2842−2847.
(35) Tømmeraas, K.; Köping-Höggård, M.; Vårum, K. M.; Christensen, B. E.; Artursson, P.; Smidsrød, O. Preparation and Characterisation of Chitosans with Oligosaccharide Branches. *Carbohydr. Res.* **2002**, *337*, 2455−2462.
(36) Freeman, R.; Hill, H. D. W.; Tomlinson, B. L.; Hall, L. D. Dipolar Contribution to NMR Spin-Lattice Relaxation of Protons. *J. Chem. Phys.* **1974**, *61*, 4466−4473.